

# Basinal Seamounts and Seamount Chains of the Central Indian Ocean: Probable Near-Axis Origin from a Fast-Spreading Ridge

RANADHIR MUKHOPADHYAY and RODEY BATIZA

*National Institute of Oceanography, Dona Paula, Goa 403004, India*

*Department of Geology and Geophysics, University of Hawaii, Honolulu, HI 96822, U.S.A.*

(Received 14 February, 1993; accepted 22 May, 1993)

**Key words:** Seamount volcanism. Central Indian Ocean.

**Abstract.** Hydrosweep mapping of crust in the Central Indian Ocean Basin reveals abundant volcanoes occurring both as isolated seamounts and linear seamount chains parallel to flow lines. Their shapes, sizes and overall style of occurrence are indistinguishable from near-axis seamounts in the Pacific. Evidence from seamount morphology, distributions and petrography of dredged samples suggests that they were generated near the fast-spreading Southeast Indian Ridge at 50–60 Ma. If so, this style of near-axis seamount generation may be a result of fast-spreading rate rather than a peculiarity of the present Pacific spreading ridges. In fact, the results of several recent studies, taken together, suggest that the style of axis/near-axis seamount volcanism varies systematically as a function of spreading rate.

## Introduction

Previous studies have shown that the distribution and style of seamount volcanic activity at or near active mid-ocean ridges varies as a function of spreading rate. At fast- and medium-spreading rates (16.0 to 5.5 cm yr<sup>-1</sup> full rate) abundant volcanoes (seamounts) are produced on the near-axis flanks of the ridge (Batiza and Vanko, 1983; Davis and Karsten, 1986; Smith and Jordan, 1988; Batiza *et al.*, 1990; Wilson, 1992; Shen *et al.*, 1993). These volcanoes exhibit an exponential size distribution (Smith, 1988), with the largest being over 2 km high. Many of those over 500 m high are demonstrably the result of many eruption episodes and have had relatively long and complex volcanic histories (Allan *et al.*, 1987; Batiza *et al.*, 1989a; Fornari *et al.*, 1988; Allan *et al.*, 1989). Only very rarely are seamounts formed exactly at the ridge

axis. Instead, they seem to form on the near-axis flanks and continue to grow as the young lithosphere moves away from the axis (Menard, 1969). Petrologic data (Batiza and Vanko, 1984; Allan *et al.*, 1987, 1989; Batiza *et al.*, 1990; Niu and Batiza, 1991) indicates that seamounts near the East Pacific Rise (EPR) are not fed by the axial magma lens nor by unusual mantle sources. Rather, seamount melts are produced in the upwelling zone of mantle that also supplies the axis. Seamounts thus appear to be a normal by-product of magmatic and tectonic activity at fast- to medium-spreading rates.

Seamounts formed near ridge axes in the Pacific commonly form linear chains oriented along flow lines and the direction of absolute plate motion (Batiza *et al.*, 1990). The latter seem to form mini hot-spot chains, but chemically they are indistinguishable from flow-line chains and do not require a distinct mantle source (Davis and Karsten, 1986; Desonie and Duncan, 1990; Wilson, 1992). The question of whether these two types of chains are a normal consequence of fast- to medium-spreading ridges or, alternatively, a tectonic peculiarity of the present Pacific ridges can be answered partly by examining ocean crust produced by other fast-spreading systems. In this study, we show that Eocene and Paleocene (50–60 Ma) crust of the Central Indian Ocean Basin, produced by the then, fast-spreading Southeast Indian Ridge (SEIR) contains numerous individual seamounts and flow-line parallel seamount chains. We conclude that such chains are the result of fast-spreading systems. Seamount chains parallel to the absolute motion of the Indian plate cannot be distinguished with confidence because the motion of the Indian plate,

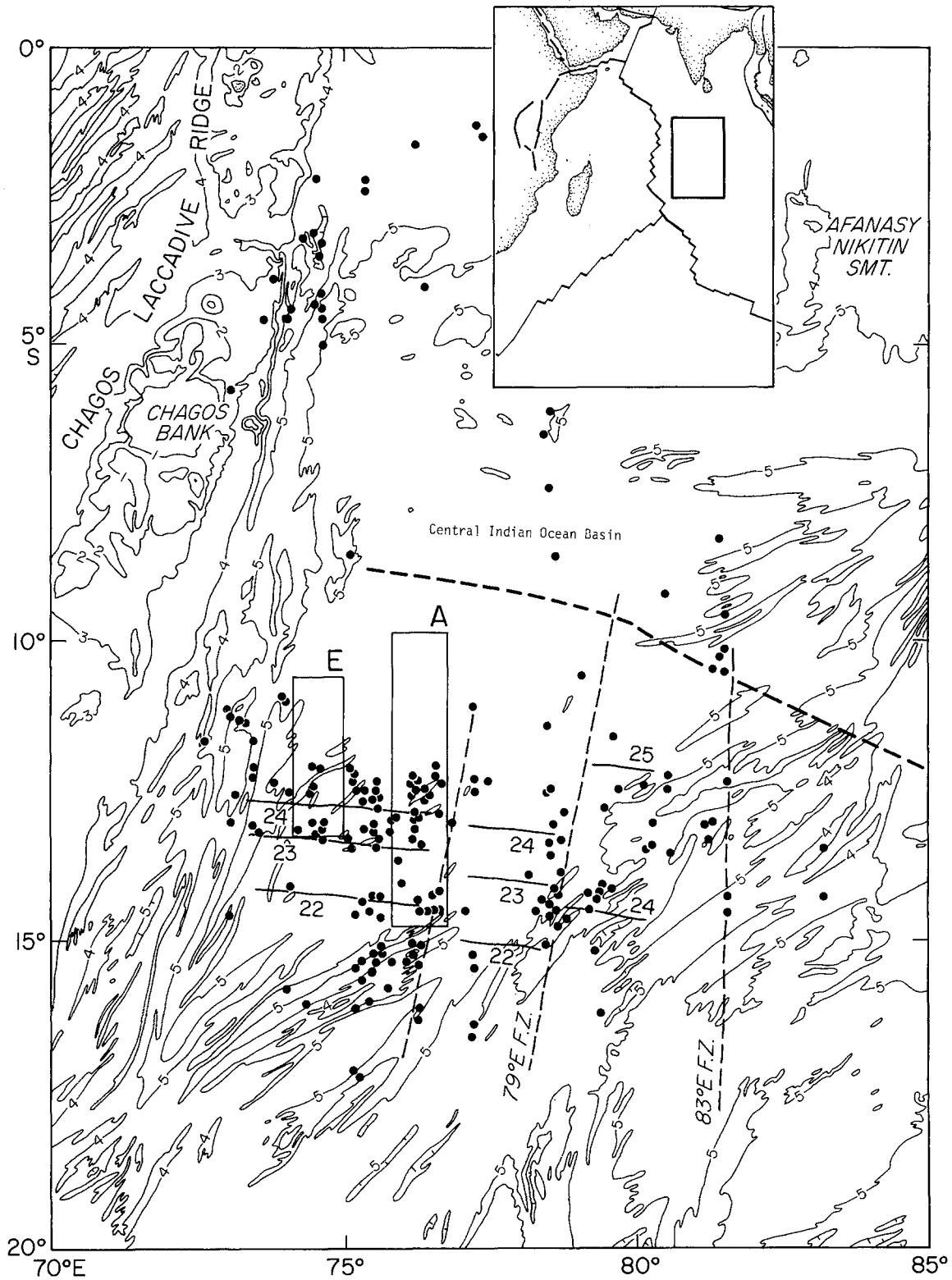


Fig. 1. Bathymetry of part of Indian Ocean (see inset) from Fisher *et al.* (1982). The Central Indian Ocean Basin is bounded on the west by the Chagos-Laccadive bank and on the east by the Ninetyeast Ridge. Boxes indicate the areas (Area A, Figure 2a and Area E, Figure 2b) surveyed with Hydrosweep. Magnetic anomalies (numbered solid lines) are from Kamesh-Raju and Ramprasad (1989) and Kamesh-Raju *et al.* (1993). Using the time scale of Kent and Gradstein (1986), the areas of Figure 2 are ~50–60 m.y.b.p. in age. The heavy dashed line is the approximate southern boundary of the area of active seismicity and deformation identified as a diffuse plate boundary zone by Petrov and Wiens (1989). The dots are seamounts, mostly identified from wide beam echo-sounder surveys (Mukhopadhyay and Khadge, 1990) and multibeam data of Kamesh-Raju *et al.* (1993).

relative to the hot-spot reference frame in Eocene-Paleocene, was very close to its direction of relative motion.

### Study Area

Figure 1 shows the portion of the Central Indian Ocean Basin (CIOB) containing the two areas with multi-beam bathymetric data we examined. The CIOB has been produced by slow-spreading of the Central Indian Ridge (CIR) and fast- to medium-spreading at the Southeast Indian Ridge (SEIR). The areas of Figures 2a and 2b were produced by the fast-spreading ( $\sim 11\text{--}15\text{ cm yr}^{-1}$  full rate) SEIR between  $\sim 60\text{--}50\text{ Ma}$ . In this region, the spreading direction (fracture zones and flow lines) is roughly North-South and ridge-parallel abyssal hills are roughly East-West. Except for the Chagos bank and the Ninetyeast Ridge, thought to have been produced by the Reunion and Kerguelen hot spots, our study area is free from identified hot spots or large hot-spot produced seamount chains.

The CIOB began forming at least 84 m.y.b.p. as India moved northward away from Antarctica (Royer *et al.*, 1992) at somewhat variable but rapid rates (Klootwijk *et al.*, 1992; Pierce, 1978). Between anomalies 22 and 26 (51.9 to 60.7 Ma; Kent and Gradstein, 1986) from Kamesh-Raju and Ramprasad (1989), spreading rates varied from  $15.1\text{--}11\text{ cm yr}^{-1}$  (full rate), as fast as many of the present Pacific spreading ridges (Macdonald, 1989; Atwater, 1989). A slowing of India's northward motion to  $10\text{--}11\text{ cm yr}^{-1}$  (full rate) occurred in the period 40–55 Ma which is inferred to represent the collisional contact between India and Asia (Klootwijk *et al.*, 1992).

Figure 1 also shows the area of deformation, high heat flow, lineated gravity and geoid anomalies and seismicity which is thought to represent the diffuse plate boundary between the Indo-Arabian and Australian plates (e.g., Wiens *et al.*, 1985; Petroy and Wiens, 1989; Royer and Chang, 1991; Geller *et al.*, 1983; Stein and Okal, 1978; Bull, 1990; Bull and Scrutton, 1990). Small-scale deformation in this area consists mostly of reactivation of inward and outward facing ridge-parallel faults forming abyssal hills (Bull and Scrutton, 1990) but appears to be restricted to the area north of  $6^\circ\text{ S}$  latitude. The timing of deformation is uncertain; it may have begun as early as 21 Ma (Royer and Chang, 1991) or as late as 5–7 Ma (Cochran *et al.*, 1987; Bull, 1990). The areas of Figure 2, though

adjacent to the zone of deformation, seem to be unaffected by it. Intraplate seismicity is present in a broad zone, however there are no epicenters located in the areas of Figure 2. Except for broadly scattered seismicity, there is no evidence for significant intraplate deformation much to the south of  $10^\circ\text{ S}$ . While we cannot preclude deformation in our study area, more detailed work on the sediments,  $\leq 100\text{ m}$  thick in this area (Udintsev *et al.*, 1975) are needed to document possible effects. To a first order; however, neither the directions of seafloor lineations nor the throws on abyssal hills' faults seem anomalous. We may thus consider that the seafloor fabric shown in Figure 2 consists of unmodified or only slightly modified ridge-generated abyssal hills and offset traces.

### Results

Figure 2 shows the two areas representing  $\sim 85000\text{ km}^2$  of seafloor mapped with complete coverage by Hydrosweep (Gutberlet and Schenke, 1989), a high resolution multibeam system installed on the ORV *Sagar Kanya* of the National Institute of Oceanography of India. The survey was carried out in 1991–1992 and was navigated using Global Positioning System (GPS) data interfaced to an Integrated Navigation System. Navigational accuracy is estimated to be within a few tens of meters. Complete bathymetric maps and detailed discussion of the geologic history of the area will be presented elsewhere (Mukhopadhyay *et al.*, in preparation).

The seamounts in the area have been categorized as major (height  $\geq 1000\text{ m}$ ), intermediate (height  $500\text{--}999\text{ m}$ ) and minor (height  $100\text{--}499\text{ m}$ ). These are listed in Table I and shown (numbered) on Figure 2. In addition, tiny volcanic cones with heights of  $50\text{--}100\text{ m}$  are also shown (unnumbered) on Figure 2. The seamounts exhibit an exponential size distribution and are mostly grouped in linear chains, trending roughly N-S, parallel to the spreading direction. Figure 3 shows bathymetric maps of three representative areas of Figure 2 with about a dozen seamounts and Figure 4 shows several seamount shape parameters plotted against seamount height.

In plan, most of the volcanoes are circular to subcircular, in many cases showing subtle to prominent elongation of the base or flat summit region. The directions of elongation tend to be mostly N-S or E-W (Figures 2, 3), however the intermediate and minor seamounts commonly show oblique

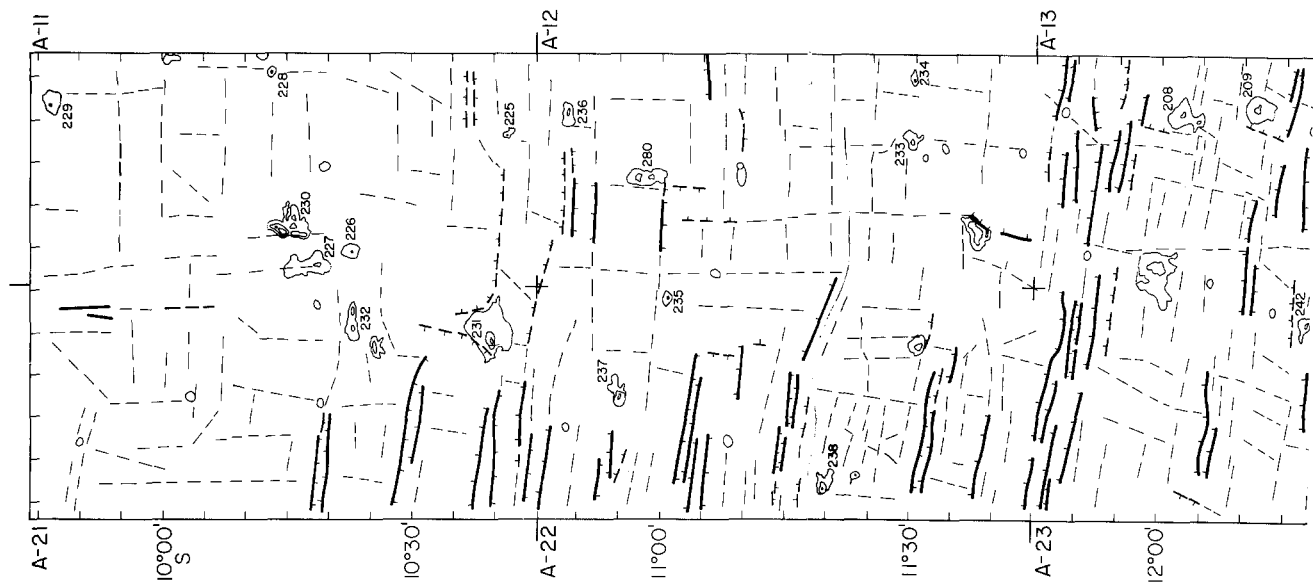


Fig. 2a

Fig. 2. See Figure 1 for location of the two areas (A and E) shown in Figures 2a and 2b. These maps were prepared from the processed Hydrosweep data and show seafloor lineations (mostly faults) and seamount locations. The regional depth in both areas is mostly 5200–5400 m and the seafloor is reasonably flat except where interrupted by faults and seamounts. Numbered seamounts (closed contour lines) are  $> 100$  m in height (see Table I) and in most cases we show contour lines for the base and flat summit region. Faults are shown with tick marks on the deep side: heavy solid lines are faults with  $\geq 100$  m of bathymetric displacement (ignoring the effect of sediment burial), dashed lines with tick marks have 100–50 m bathymetric displacement and thin dashed lines have less than 50 m displacement. In some cases, the thin dashed lines represent the trends of straight contour lines. Note the occurrence of numerous linear seamount chains striking mostly parallel to flow-line seafloor fabric (roughly N-S). In other cases, seamount elongation or short chains trend roughly East-West (ridge-parallel). Isolated seamounts, particularly small ones, are also present, however there are no clear examples of chains trending at oblique angles to the seafloor fabric.

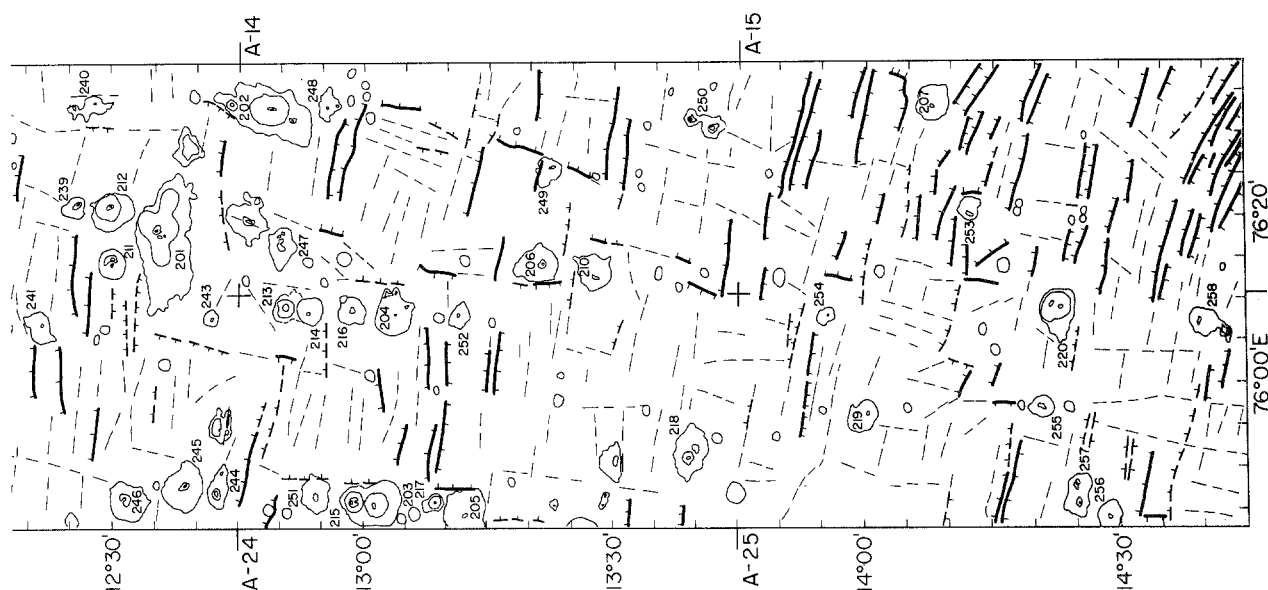
elongations (NW-SE and NE-SW). About half of the major and intermediate size seamounts have craters on their flat summits. Some of the largest seamounts consist of several coalesced edifices with curvilinear ridges resembling small lateral rift zones (see, e.g., Figure 3). Commonly, individual steep-sided, flat-topped edifices are superposed on the sides of preexisting constructions, showing that the initial stages of growth were from distributed conduits. In profile, the larger volcanoes resemble flat-topped Galapagos volcanoes with upward-steepening slopes (Simkin, 1984). Morphologically, the seamounts thus closely resemble near-axis volcanoes in the Pacific (e.g., Batiza and Vanko, 1983) which share the above features. Also like the Pacific, the Indian Ocean seamounts occur singly and in short linear chains of three to more than ten individual edifices.

The distribution of seamounts within the two mapped areas is patchy. In the eastern area, Area A (Figure 2a), seamounts are most abundant south of about  $12^{\circ}$  S. It is possible that greater sediment thickness in the northern part of the area has buried

a larger proportion of seamounts. In general, seafloor topography is more subdued in the north, providing support for this idea. However in the western area (Area E – Figure 2b) there are numerous seamounts north of  $12^{\circ}$  N. Thus, we conclude that while sediment burial has probably modified the apparent seamount distributions, the distribution is essentially nonuniform. Seamounts locally cover about 3% of the crust in the surveyed areas but abundances within subareas vary from 0.3% to 10.1%. The seamounts in this part of the CIOB resemble Pacific near-axis seamounts in size, size distribution, morphology and mode of occurrence. Thus, although their ages are presently unknown ( $^{40}\text{Ar}/^{39}\text{Ar}$  dating in progress), we conclude that they represent ancient (50–60 Ma) seamounts generated near the axis of the Southeast Indian Ridge.

## Discussion

While seamount morphology, size distribution and occurrence in flow-line parallel chains all favor the interpretation that the seamounts were generated



by the fast-spreading SEIR, an alternative interpretation is that the seamounts are much younger than the crust they are built on and perhaps formed as a result of intraplate deformation of the CIOB sometime in the Miocene. Even though the best-documented and most intense deformation occurs north of  $10^{\circ}$  S, we cannot completely rule out the possibility of some deformation occurring in the  $10^{\circ}$  S– $15^{\circ}$  S area. Such deformation could result not only in the formation of new seamounts but also additions to preexisting ones.

Another line of evidence for a near-axis origin comes from petrographic study of basalts dredged from seamounts 202, 248, 204 and others (Table I, Figure 2). While chemical analyses are not available (XRF and electron microprobe analyses are in progress and will be published separately), the samples are petrographically identical to depleted tholeiite (normal mid-ocean ridge basalt) dredged from many near-axis seamounts in the Pacific. All samples are coated with manganese and slightly to moderately altered. The rocks are non-vesicular, and most have sparse phenocrysts (or pseudo-

morphs) of olivine and plagioclase. Some samples have small subhedral sector-zoned crystals of clinopyroxene. Texturally, the samples are indistinguishable from N-MORB, and are quite different from alkalic basalts, basanites or even more undersaturated basalts expected for small intraplate eruptions. While many lines of evidence point to a near-axis origin, a key test for this hypothesis will be the results of radiometric dating.

If the seamounts were, in fact, generated near axis, then it is interesting that unlike the Pacific, there is an apparent absence of absolute motion parallel chains. Such chains are abundant at the Juan de Fuca Ridge as well as the northern and southern East Pacific Rise (e.g., Davis and Karsten, 1986; Desonie and Duncan, 1990; Batiza *et al.*, 1990; Shen *et al.*, 1993). However the absolute motion of the CIOB in Lower Eocene to Upper Paleocene time was very similar to its relative motion (Gordon and Jurdy, 1986; Duncan and Richards, 1991), a situation not unlike that of the present southern East Pacific Rise. It is thus difficult to distinguish flow line parallel from absolute

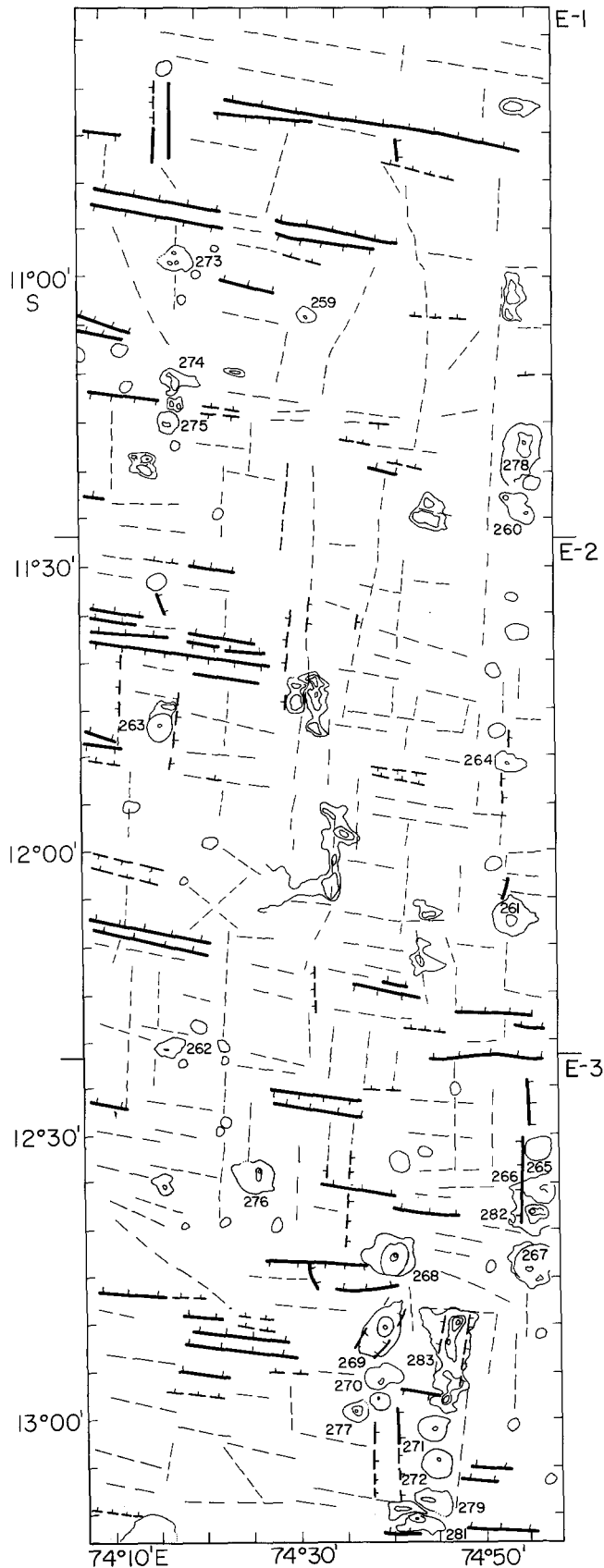


Fig. 2b

motion-parallel chains in the CIOB. On the basis of the close similarity between young near-axis seamounts in the Pacific and their ancient counterparts in the CIOB, we conclude that the abundant production of near-axis seamounts is not a peculiarity of the Pacific but is a common feature of fast- and medium-spreading ridges.

In contrast with fast- to medium-spreading ridges, slow-spreading ridges like the northern Mid-Atlantic Ridge seem to produce extremely abundant but smaller (monogenetic?) cones, many of which form exactly at the neovolcanic zone (Smith and Cann, 1992). Most large seamounts on the flanks of the Mid-Atlantic Ridge may be hot-spot related (e.g., Epp and Smoot, 1989; Cherkis *et al.*, 1992). The southern Mid-Atlantic Ridge, spreading at slow to medium rates ( $3.5 \text{ cm yr}^{-1}$  full rate: Grindlay *et al.*, 1992) produces small edifices similar to those of the northern Mid-Atlantic Ridge, plus larger Pacific-type edifices (Batiza *et al.*, 1989b). It is not clear, however, whether these larger seamounts originate within the neovolcanic zone or at some distance away. Thus, while the shapes of seamounts appear to be independent of spreading rate (Smith and Cann, 1992), the overall style of axial and near-axis seamount volcanism seems to vary systematically as a function of spreading rate.

#### Acknowledgments

We gratefully acknowledge the support of CSIR and DOD (India) and NSF and ONR (USA). We especially thank G. Ranade, P. George and T. Sudhakar for hydrosweep operation and generation of several maps onboard using EPR 1300 computer. We thank B. Bays and B. Taylor for making the figures and two reviewers whose comments improved the paper. This is SOEST contribution 3179. This work was carried out while RM was on a Raman Fellowship at UH.

TABLE I  
Seamounts of the Central Indian Ocean

Seamount Number	Area	Water Depth (m)	Height (m)	Basal Area (sq. km)	Summit Area (sq. km)	Volume (cu. km)	Flatness	Slope angle (degrees)
<i>Area A</i>								
201	13	5375	1201	236	1.0	101.0	0.07	8.4
202	14	5400	1076	163	0.2	60.6	0.04	8.8
203	24	5300	1101	94	0.9	38.2	0.10	12.6
204	24	5400	1125	58	0.3	23.4	0.07	15.8
205	24	5275	1250	90	0.6	40.8	0.08	14.3
206	14	5350	1025	80	0.2	28.8	0.05	12.1
207	15	5200	1051	67	0.8	26.3	0.11	14.3
208	13	5400	525	22	0.7	4.7	0.18	13.6
209	13	5425	600	36	1.5	9.0	0.20	12.6
210	14	5425	725	46	0.2	11.9	0.07	11.5
211	13	5400	625	40	0.3	9.1	0.09	10.9
212	13	5400	925	65	0.8	22.5	0.11	12.9
213	24	5375	600	27	0.2	5.9	0.09	12.6
214	24	5375	650	37	0.5	9.1	0.12	12.1
215	24	5300	625	36	0.3	8.2	0.09	11.5
216	24	5375	850	25	0.1	7.6	0.06	17.8
217	24	5200	575	44	0.2	9.0	0.07	9.4
218	24	5400	850	80	0.3	24.1	0.06	10.2
219	25	5200	750	34	0.3	9.4	0.09	14.1
220	25	5300	725	75	0.5	19.7	0.08	9.2
225	11	5350	100	4	0.2	0.2	0.22	6.5
226	11	5325	250	15	0.2	1.4	0.12	7.4
227	11	5325	125	4	0.1	0.2	0.16	7.5
228	11	5400	100	3	0.3	0.1	0.32	8.5
229	11	5425	100	16	0.3	0.6	0.14	2.9
230	11	5350	125	23	0.04	1.0	0.04	2.8
231	21	5300	200	107	1.0	7.9	0.10	2.2
232	21	5350	100	24	0.4	0.9	0.13	2.4
233	12	5425	300	13	0.3	1.5	0.15	9.9
234	12	5375	150	15	0.2	0.8	0.12	4.4
235	12	5375	125	5	0.1	0.2	0.14	6.6
236	12	5325	150	14	0.6	0.9	0.21	5.1
237	22	5200	126	24	0.4	1.2	0.13	3.0
238	22	5300	175	16	0.1	1.0	0.08	4.8
239	13	5400	255	28	0.3	2.7	0.10	5.4
240	13	5300	130	31	0.3	1.5	0.10	2.6
241	23	5300	530	34	0.2	6.5	0.08	9.9
242	23	5325	355	8	0.2	1.1	0.16	14.8
243	23	5300	205	11	0.4	0.9	0.19	7.7
244	23	5300	330	48	0.9	6.1	0.14	5.6
245	23	5300	430	101	0.3	15.3	0.05	4.6
246	23	5300	810	64	0.4	18.8	0.08	11.0
247	14	5300	230	37	2.6	3.8	0.27	5.2
248	14	5300	355	26	0.3	3.4	0.11	7.9
249	14	5400	410	21	0.2	3.2	0.10	10.0
250	14	5400	230	79	0.6	6.6	0.09	2.9
251	24	5300	255	58	0.8	5.6	0.12	3.8
252	24	5300	255	21	0.4	2.1	0.14	6.5
253	15	5200	300	22	0.0	2.2	0.00	6.5
254	25	5250	375	63	0.2	8.3	0.06	5.1
255	25	5215	460	37	1.5	7.0	0.20	9.5
256	25	5200	480	19	0.9	3.8	0.22	14.0
257	25	5200	380	49	0.6	7.0	0.11	6.2
258	25	5200	280	49	0.3	5.0	0.08	4.4
280	12	5400	100	25	1.0	1.0	0.20	2.5

TABLE I (Cont.)

## Seamounts of the Central Indian Ocean

Seamount Number	Area	Water Depth (m)	Height (m)	Basal Area (sq. km)	Summit Area (sq. km)	Volume (cu. km)	Flatness	Slope angle (degrees)
<i>Area E</i>								
259	1	5100	180	6	0.2	0.4	0.18	9.1
260	1	5100	130	27	1.0	1.4	0.19	3.1
261	2	5200	682	24	0.2	6.0	0.09	15.2
262	2	5000	155	11	0.4	0.7	0.19	5.8
263	2	5100	410	12	0.2	1.9	0.13	13.5
264	2	5175	250	7	0.3	0.7	0.21	11.9
265	3	5200	230	7	0.2	0.6	0.17	10.5
266	3	5200	480	18	0.4	3.4	0.15	13.3
267	3	5200	710	30	0.4	8.0	0.12	14.6
268	3	5100	460	51	0.2	8.3	0.06	6.9
269	3	5100	530	39	0.2	7.4	0.07	9.2
270	3	5100	480	16	0.4	3.0	0.16	14.2
271	3	5200	430	17	0.4	2.9	0.15	12.3
272	3	5200	530	21	0.3	4.2	0.12	13.1
273	1	5100	150	21	0.3	1.2	0.12	3.8
274	1	5100	175	21	0.2	1.4	0.10	4.3
275	1	5100	200	13	0.5	1.1	0.20	7.0
276	3	5000	250	38	1.4	3.9	0.19	5.1
277	3	5400	200	13	2.1	1.4	0.40	9.3
278	1	5200	150	60	9.5	4.7	0.40	3.3
279	3	5100	175	27	1.3	2.0	0.22	4.4
280	12	5400	100	25	1.0	1.0	0.20	2.5
281	3	5100	225	40	0.2	3.2	0.07	3.9
282	3	5200	400	13	2.1	2.7	0.40	18.2
283	3	5275	175	83	3.6	6.1	0.21	2.5

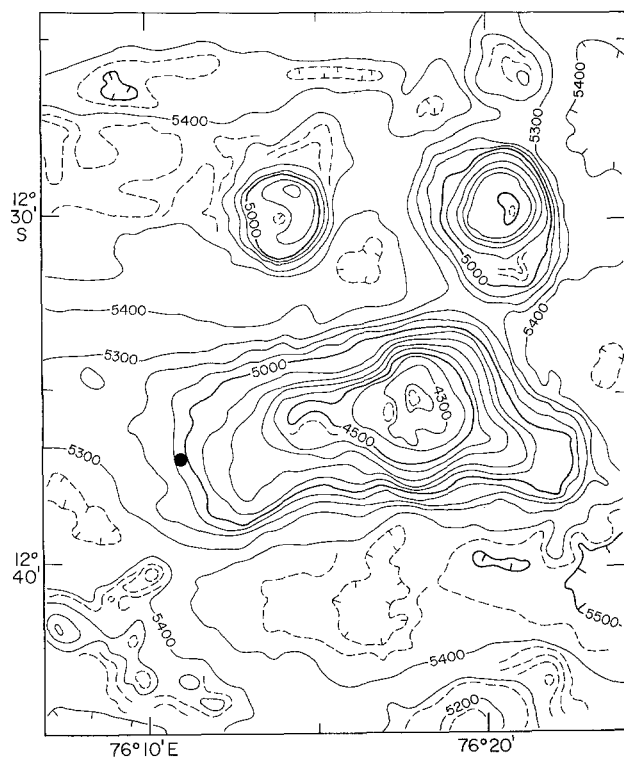


Fig. 3a

Fig. 3. Bathymetric maps of three small areas of Figure 2 showing representative seamounts. Contour interval (solid lines) is 100 m with some 25 m contours dashed. (a) The largest seamount (#201) is elongated E-W and consists of two coalesced edifices. Note the volcanic ridge extending eastward and the dredge site (dot). The largest seamount is also part of a short N-S chain of three edifices. (b) two *en-echelon* N-S seamount chains. (c) a short N-S chain consisting of a tall (700 m high), steep-sided and flat-topped edifice and two edifices with gentler slopes.



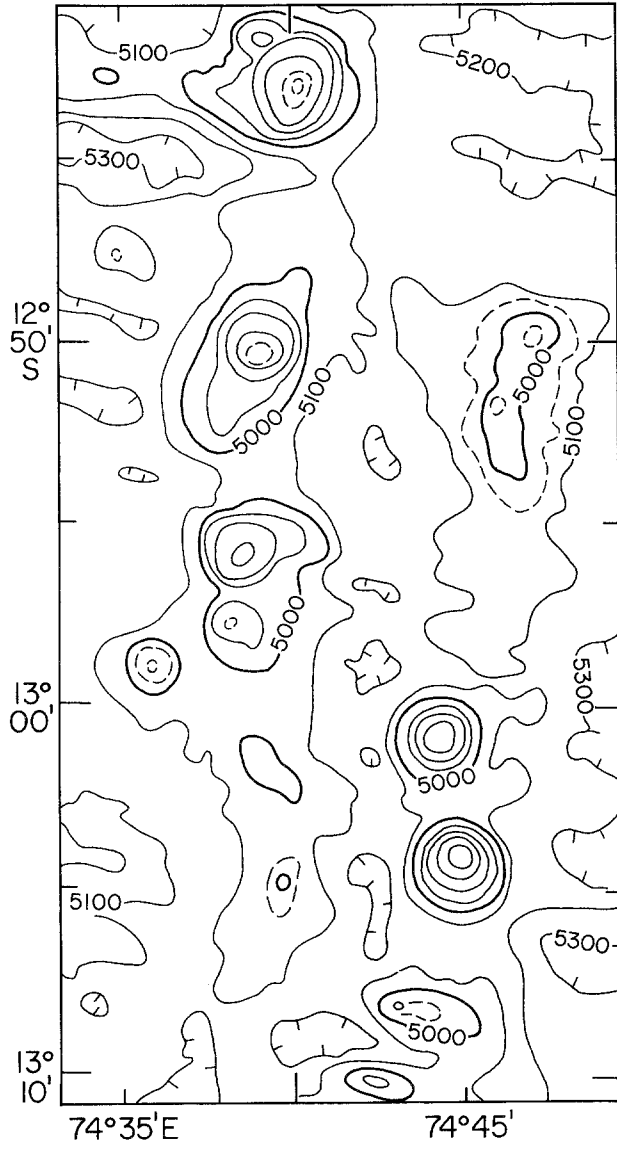


Fig. 3b.

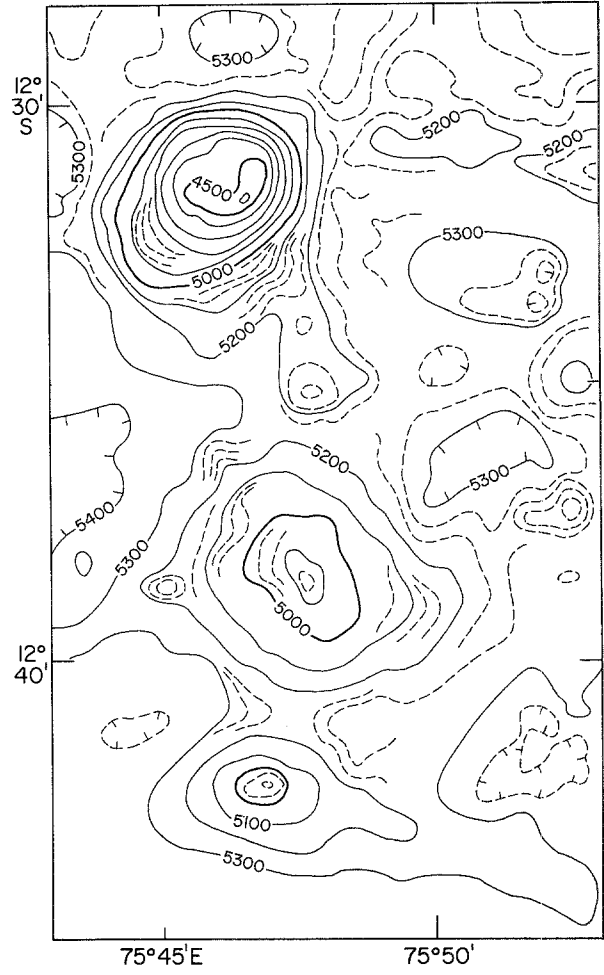


Fig. 3c.

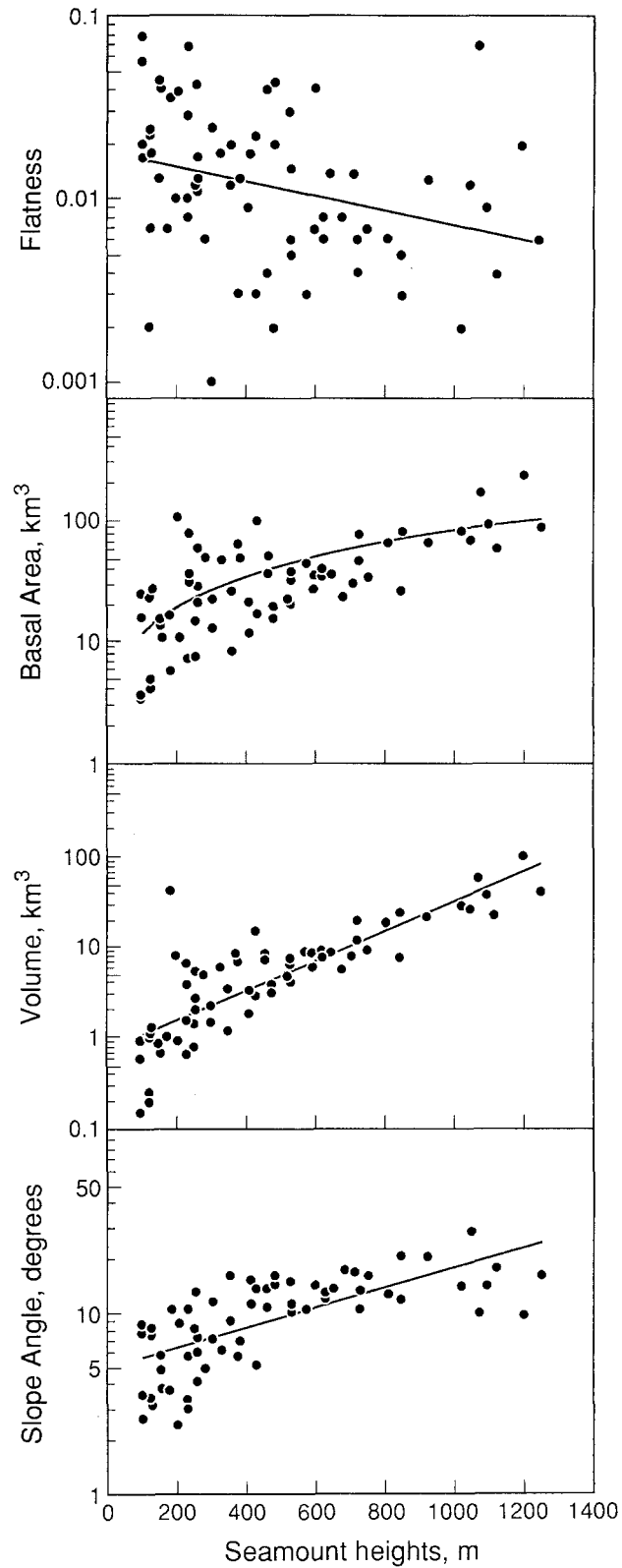


Fig. 4. Data from Table I shown graphically. Flatness ( $r_s/r_b$ ), basal area, volume and slope angle plotted against seamount height. These patterns of variation are similar to those observed for Pacific near-axis seamounts.

## References

- Allan, J. F., Batiza, R., and Lonsdale, P., 1987, Petrology of Lavas from Seamounts Flanking the East Pacific Rise, 21° N: Implications Concerning the Mantle Source Compositions for Both Seamounts and the Adjacent EPR Lavas, in B. H. Keating, P. Fryer, R. Batiza, and G. Boehlert (eds), *Seamounts, Islands and Atolls*, AGU Geophysical Monograph **43**, 255–282.
- Allan, J. F., Batiza, R., Perfit, M. R., Fornari, D. J., and Sack, R. O., 1989, Petrology of Lavas from the Lamont Seamount Chain and Adjacent East Pacific Rise, 10° N, *J. Petrol.* **30**, 1245–1298.
- Atwater, R., 1989, Plate Tectonic History of the Northeast Pacific and Western North America, in *The Geology of North America*, vol. N, 21–72.
- Batiza, R. and Vanko, D., 1983, Volcanic Development of Small Oceanic Central Volcanoes on the Flanks of the East Pacific Rise Inferred from Narrow Beam Echo Sounder Surveys, *Mar. Geol.* **54**, 53–90.
- Batiza, R. and Vanko, D., 1984, Petrology of Pacific Seamounts, *J. Geophys. Res.* **89**, 11235–11260.
- Batiza, R., Smith, T., and Niu, Y., 1989a, Geologic and Petrologic Evolution of Seamounts Near the EPR Based on Submersible and Camera Study, *Mar. Geophys. Res.* **11**, 169–236.
- Batiza, R., Fox, P. J., Vogt, P. R., Cande, S. C., and Grindlay, N. R., 1989b, Abundant Pacific-type Near-ridge Seamounts in the Vicinity of the Mid-Atlantic Ridge 26° S, *J. Geol.* **97**, 209–220.
- Batiza, R., Niu, Y., and Zayac, W. C., 1990, Chemistry of Seamounts Near the East Pacific Rise: Implications for the Geometry of Sub-acid Mantle Flow, *Geology* **18**, 1122–1125.
- Bull, J. M., 1990, Structural style of intra-plate deformation, Central Indian Ocean Basin: Evidence for the role of fracture zones, *Tectonophysics* **184**, 213–228.
- Bull, J. M. and Scrutton, R. A., 1990, Fault Reactivation in the Central Indian Ocean and the Rheology of Oceanic Lithosphere, *Nature* **344**, 855–858.
- Cherkis, N. Z., Chayes, D. A., and Costa, L. C., 1992, The Bathymetry Distribution of the Bahia Seamounts, Brazil Basin, *Mar. Geol.* **103**, 335–347.
- Cochran, J. R. and Leg 116 shipboard scientific party, 1987, Ocean Drilling Program, Collisions in the Indian Ocean, *Nature* **330**, 519–521.
- Davis, E. E. and Karsten, J. L., 1986, On the Cause of Asymmetric Distribution of Seamounts about the Juan de Fuca Ridge: Ridge Crest Migration over a Heterogeneous Asthenosphere, *Earth Planet. Sci. Lett.* **79**, 385–396.
- Desonie, D. L. and R. A. Duncan, 1990, The Cobb-Eichelberg Seamount Chain: Hotspot Volcanism with Mid-ocean Ridge Basalt Affinity, *J. Geophys. Res.* **95**, 12,697–12,712.
- Duncan, R. A. and Richards, M. A., 1991, Hotspots, Mantle Plumes, Flood Basalts and True Polar Wonder, *Reviews of Geophysics* **29**, 31–50.
- Epp, D. and Smoot, N. C., 1989, Distribution of Seamounts in the North Atlantic, *Nature* **337**, 254–257.
- Fisher, R. L., Jantsch, M. Z., and Comer, R. L., 1982, General Bathymetric Chart of the Oceans (GEBCO) Sheet 5–09.
- Fornari, D. J., Perfit, M. R., Allan, J. F., Batiza, R., Hayman, R., Barone, A., Ryan, W. B. F., Smith, T., and Simkin, T., 1988, Seamounts as Windows into Mantle Processes: Structural and Geochemical Studies of the Lamont Seamounts, *Earth Planet. Sci. Lett.* **89**, 63–83.
- Geller, C. A., Weissel, J. K., and Anderson, R. N., 1983, Heat Transfer and Intraplate Deformation in the Central Indian Ocean, *J. Geophys. Res.* **88**, 1018–1032.
- Gordon, R. G. and Jurdy, D. M., 1986, Cenozoic Global Plate Motions, *J. Geophys. Res.* **91**, 12,289–12,406.
- Grindlay, N. R., Fox, R. J., and Vogt, P. R., 1992, Morphology and Tectonics of the Mid-Atlantic Ridge (25°–27°30' S) from Seabeam and Magnetic Data, *J. Geophys. Res.* **97**, 6983–7010.
- Gutberlet, M. and Schenke, H. W., 1989, Hydrosweep: New Era in High Precision Bathymetric Surveying in Deep and Shallow Water, *Mar. Geodesy* **13**, 1–23.
- Kamesh-Raju, K. A. and Ramprasad, T., 1989, Magnetic Lineations in the Central Indian Basin for the Period A24–A21: A Study in Relation to the Indian Ocean Triple Junction Trace, *Earth Planet. Sci. Lett.* **95**, 395–402.
- Kamesh-Raju, K. A., Ramprasad, T., Kodagali, V. N., and Nais, R. R., 1993, Multibeam Bathymetry, Gravity and Magnetic Studies over 79° E Fracture Zone–Central Indian Basin, *J. Geophys. Res.* (in press).
- Kent, D. V. and Gradstein, F. M., 1986, A Jurassic to Recent Chronology, in *The Geology of North America*, vol. N, 45–50.
- Klootwijk, C. T., Gee, J. S., Peirce, J. W., Smith, G. M., and McFadden, P. L., 1992, An Early India-Asia Contact: Paleomagnetic Constraints from Ninetyeast Ridge, ODP Leg 121, *Geology* **20**, 395–398.
- Macdonald, K. C., 1989, Tectonic and Magmatic Processes on the East Pacific Rise, in *The Geology of North America*, vol. N, 93–110.
- Menard, H. W., 1969, Growth of Drifting Volcanoes, *J. Geophys. Res.* **74**, 4827–4837.
- Mukhopadhyay, R., and Khadge, N. H., 1990, Seamounts in the Central Indian Ocean Basin: Indicators of the Indian Plate Movement, *Proc. Indian Acad. Sci.* **99**, 357–365.
- Niu, Y. and Batiza, R., 1991, An Empirical Method of Calculating Melt Compositions Produced beneath Mid-Ocean Ridges: Application for Axis and Off-axis (Seamounts) Melting, *J. Geophys. Res.* **96**, 21753–21777.
- Peirce, J. W., 1978, The Northward Motion of India since the Late Cretaceous, *Roy. Astr. Soc. Geophys. J.* **52**, 277–311.
- Petroy, D. E. and Wiens, D. A., 1989, Historical Seismicity and Implications for Diffuse Plate Convergence in the Northeast Indian Ocean, *J. Geophys. Res.* **94**, 12,301–12,319.
- Royer, J.-Y. and Chang, T., 1991, Evidence for Relative Motion between the Indian and Australian Plates during the Last 20 m.y. from Plate Tectonic Reconstructions: Implications for Deformation of the Indo-Australian Plate, *J. Geophys. Res.* **96**, 11,779–11,802.
- Royer, J.-Y., Sclater, J. G., Sandwell, D. T., Londe, S. C., Schlich, R., Munsch, M., Dymment, J., Fisher, L., Muller, R. D., Coffins, M. F., Patriat, P., and Bergh, H. W., 1992, Indian Ocean Plate Reconstructions since the Late Jurassic, in R. A. Duncan *et al.* (eds) *A Synthesis of Scientific Drilling Results from the Indian Ocean*, Amer. Geophys. U. Monograph 70 (Washington, D. C.).
- Shen, Y., Forsyth, D. W., Scheirer, D. S., and Macdonald, K. C., 1993, Two Forms of Volcanism: Implications for the Volume of Off-axis Crustal Production on the West Flank of the East Pacific Rise, *J. Geophys. Res.* (in press).

- Simkin, T., 1984, The Geology of the Galapagos Islands, in R. Perry (ed). *The Galapagos*, Pergamon Press, Oxford, 15–41.
- Smith, D. K., 1988, Shape Analysis of Pacific Seamounts, *Earth Planet. Sci. Lett.* **90**, 457–466.
- Smith, D. K. and Jordan, T. H., 1988, Seamount Statistics in the Pacific Ocean, *J. Geophys. Res.* **93**, 2899–2918.
- Smith, D. K. and Cann, J. R., 1992, The Role of Seamount Volcanism in Crustal Construction at the Mid-Atlantic Ridge (24°–30° N), *J. Geophys. Res.* **97**, 1645–1658.
- Stein, S. and Okal, E. A., 1978, Seismicity and Tectonics of the Ninetyeast Ridge Area: Evidence for Internal Deformation of the Indian Plate. *J. Geophys. Res.* **83**, 2233–2246.
- Udintsev, G. B. (ed), 1975, *Geological and Geophysical Atlas of the Indian Ocean*, Acad. Sci. USSR, Moscow, 151 p.
- Wiens, D. A., DeMets, D. C., Gordon, R. G., Stein, S., Argus, D., Engeln, J. F., Lundgren, P., Quible, D., Stein, C., Wiens, S., and Woods, D. F., 1985, A Diffuse Plate Boundary Model for Indian Ocean Tectonics, *Geophys. Res. Lett.* **12**, 429–432.
- Wilson, D. S., 1992, Focussed Mantle Upwelling Beneath Mid-Ocean Ridges: Evidence from Seamount Formation and Isostatic Compensation of Topography, *Earth Planet. Sci. Lett.* **113**, 41–55.